Printed ISSN 1330–0016
Online ISSN 1333–9133
CD ISSN 1333–8390
CODEN FIZBE7

EXCLUSIVE PION ELECTROPRODUCTION OFF NUCLEONS AND NUCLEI

MURAT M. KASKULOV and ULRICH MOSEL

Institut für Theoretische Physik, Universität Giessen, D-35392 Giessen, Germany
E-mail address: murat.kaskulov@theo.physik.uni-giessen.de

Received 7 February 2011; Accepted 14 December 2011
Online 18 February 2012

We present our results for the exclusive electroproduction of pions off nucleons and nuclei at high values of Q^2. In electroproduction of nuclei $A(e, e'\pi)$ we consider the color transparency (CT) effect recently observed at JLAB. It is shown that the description of π production off nucleons is mandatory for the proof of the CT signal at JLAB. We further develop the models for exclusive production of π off nucleons at JLAB and HERMES. We first describe a model based on exclusive-inclusive connection. In the second approach, we combine a Regge pole approach with the residual effect of nucleon resonances. The nucleon resonances are described using a dual connection between the exclusive form factors and inclusive deep inelastic structure functions. We present the results for the beam spin azimuthal asymmetries measured at JLAB in exclusive electroproduction of charged and neutral pions.

PACS numbers: 12.39.Fe, 13.40.Gp, 13.60.Le, 14.20.Dh UDC 539.126, 539.171
Keywords: exclusive electroproduction of pions, nucleon and nuclear targets, high Q^2, color transparency effect, exclusive-inclusive connection model, Regge pole approach, beam spin azimuthal asymmetries

1. Introduction

Electroproduction of mesons in the deep inelastic scattering (DIS), $\sqrt{s} > 2$ GeV and $Q^2 > 1$ GeV^2, is a modern tool which permits to study the structure of the nucleon on the partonic level. Exclusive channels in DIS are of particular importance. In this kind of hard processes one may learn about the off-forward parton distributions that parameterize an intrinsic nonperturbative pattern of the nucleon, see Ref. [1] and references therein. Much work have been done to understand the production of pions in exclusive kinematics. For instance, in QCD at large values of $(\sqrt{s}, Q^2)$ and finite value of Bjorken $x_{\rm B}$, the description of $N(e, e'\pi)N'$ relies on the

dominance of the longitudinal cross section $\sigma_{\rm L}$ [2]. The transverse part $\sigma_{\rm T}$ is predicted to be suppressed by power of $\sim 1/Q^2$. However, the kinematic domain where this power suppresion dominates is not yet known for π production. A somewhat different concept is used in Regge pole models which rely on effective hadronic degrees of freedom. Here the exclusive (γ^*, π) forward production mechanism is given by the sum of all possible t-channel meson-exchange processes. Although both partonic and Regge descriptions are presumably dual, the exclusive reactions have a potential to discriminate between different models.

Related experimental studies have been carried out at JLAB [3, 4] and at HERMES/DESY [5]. A dedicated program on exclusive production of pions is planned in the future at the JLAB upgrade.

On the experimental side, it is tempting to see an onset of $\sigma_{\rm L}/\sigma_{\rm T} \propto Q^2$ scaling at presently available energies. However, the high Q^2 data from JLAB and single spin asymmetries measured in true DIS events at HERMES [6] show nonvanishing transverse components in $p(\gamma^*, \pi^+)n$. At JLAB [3, 7, 10, 11], DESY [12 – 14], Cornell [15 – 17] and CEA [18], the high Q^2 region is dominated by the conversion of transverse photons in $\sigma_{\rm T}$. For instance, the Q^2 dependence of the partial $\sigma_{\rm L}$ and $\sigma_{\rm T}$ cross sections in the π^+ electroproduction above $\sqrt{s} > 2$ GeV has been studied in Ref. [3]. In the charged pion case, the longitudinal cross section $\sigma_{\rm L}$ at forward angles is well described by the quasi-elastic π knockout mechanism [19, 20]. It is driven by the pion charge form factor [21, 22] both at JLAB and HERMES. On the contrary, the $(\sqrt{s}, Q^2)$ behavior of $\sigma_{\rm T}$ remains to be puzzling. The data demonstrate that $\sigma_{\rm T}$ is large and tends to increase relative to $\sigma_{\rm L}$ as a function of Q^2. Interestingly, the $(\sqrt{s}, Q^2)$ dependence of exclusive $\sigma_{\rm T}$ exhibits features similar to that in $p(e, e'\pi^+)X$ semi-inclusive cross sections in DIS in the limit $z \to 1$ [23, 24]. This kind of an exclusive-inclusive connection [25] has been also observed in exclusive (γ^*, ρ^0) production [26]. On the theoretical side, hadronic models based on the meson-exchange scenario alone largely underestimate the measured $\sigma_{\rm T}$ in electroproduction, see Ref. [11] for further discussions and references therein.

We have shown in Refs. [23, 27] a possible solution to the $\sigma_{\rm T}$ problem. The description of charged pion production proposed in Ref. [27] relies on the residual contribution of the nucleon resonances. It is supposed that the excitations of nucleon resonances dominate in electroproduction. The resonances are dual to the direct partonic interactions due to the Bloom-Gilman duality connection and, correspondingly, their form factors are determined by parton distribution functions. The $s(u)$-channel resonances supplement the reggeon exchanges in the t-channel. Therefore, one distinguishes peripheral t-channel meson-exchange processes and the $s(u)$-channel resonance/partonic contributions. In this way all data collected so far in the charged pion electoproduction $(e, e'\pi^\pm)$ at JLAB, DESY, Cornell and CEA can be well described [27].

A closely related phenomenon is the color transparency (CT). It becomes effective in (semi)exclusive electroproduction of mesons off nuclei, see Ref. [30] for a possible observation and Refs. [31 – 33] for further interpretations of the CT signal in the reaction $A(e, e'\pi^+)$.

2. *Color transparency in semi-exclusive reaction* $(e, e'\pi^+)$ *off nuclei*

The interactions of high-energy virtual photons with nuclei provide an important tool to study the early stage of hadronization and (pre)hadronic final-state-interactions (FSI) at small distances, $d \sim 1/\sqrt{Q^2}$. One believes that at high values of Q^2, the exclusive pions are produced in point like configurations which may interact in the nuclear medium only weakly. Thus, in the presence of the CT effect, the intranuclear attenuation of hadrons propagating through the nuclear medium should decrease as a function of photon virtuality Q^2. In this case, the nucleus becomes more transparent for the outgoing particles as compared to the case where the attenuation is driven by ordinary absorption mechanisms. At JLAB [30], the nuclear transparency[1] in semi-exclusive π^+ electroproduction reaction $A(e, e'\pi^+)$ has been measured as a function of Q^2 and the atomic mass number A. A rise of pionic transparency has been indeed observed for values of Q^2 between 1 and 5 GeV^2, see Fig. 1.

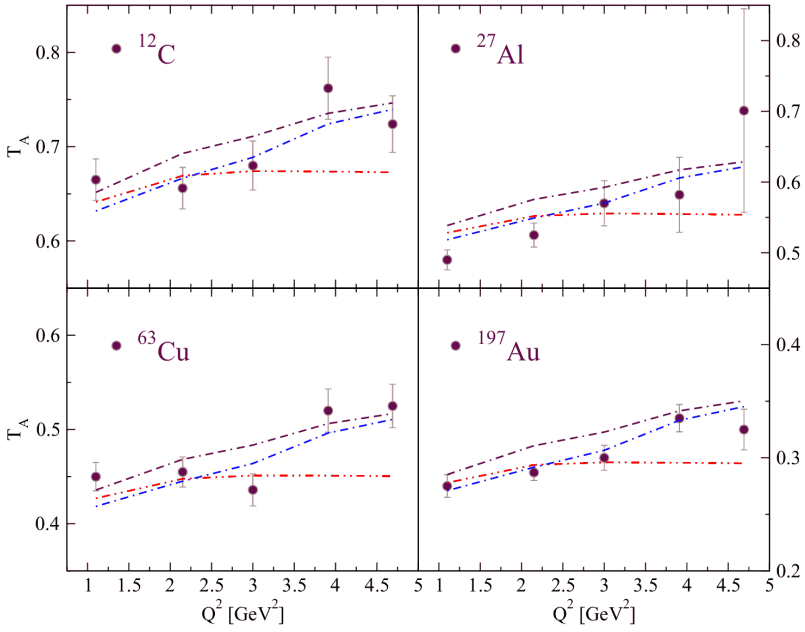

Fig. 1. Transparency, T_A, vs. Q^2 for ^{12}C (left, top panel), ^{27}Al (right, top), ^{63}Cu (left, bottom) and ^{197}Au (right, bottom). The dash-dash-dotted curves realize the CT effect in both the longitudinal and transverse channels and dash-dotted curves in the transverse channel only. The dot-dot-dashed curves describe the CT effect in the longitudinal channel only. The experimental data are from Ref. [30].

[1]The nuclear transparency for a certain reaction process is usually defined as the ratio of the nuclear cross section per target nucleon to the one for a free nucleon, i.e. $T_A = (\sigma_A/A)\sigma_N$.

In the work of Ref. [33], we have studied the onset of CT at JLAB using a factorization of the whole reaction into an initial, primary interaction of the incoming virtual photon with the nucleon and the FSI. Following the model of Ref. [23], the cross section for the former is reproduced both in its longitudinal and its transverse contribution, while the FSI is treated within the transport approach. Here the propagation of the produced (pre)hadron through the nuclear medium is described by the Boltzmann-Uehling-Uhlenbeck (BUU) equation which describes the time evolution of the phase-space density $f_i(\vec{r},\vec{p},t)$ of particles of type i that can interact via binary reactions. Besides the produced hadron and the nucleons, these particles involve the baryonic resonances and mesons that can be produced in FSI. For the baryons, the equation contains a mean field potential which depends on the particle position and momentum. The BUU equations of each particle species i are coupled via the mean field and the collision integral. The latter allows for elastic and inelastic rescattering and side-feeding through coupled-channel effects; it accounts for the creation and annihilation of particles of type i in a secondary collisions as well as elastic scattering from one position in phase space into another. The resulting system of coupled differential-integral equations is solved via a test particle ansatz for the phase space density. For fermions, Pauli blocking is taken into account via blocking factors in the collision term [34].

We use the quantum diffusion model of Ref. [35] to describe the time - development of the interactions of a point-like configuration produced in a hard initial reaction. This approach combines a linear increase of the hadron-nucleon cross section with the assumption that the cross section for the leading particles does not start at zero, but at a finite pedestal value connected with Q^2 of the initial interaction, i.e.

$$\sigma^*(t)/\sigma = X_0 + (1 - X_0)\left((t - t_P)/(t_F - t_P)\right), \tag{1}$$

where $X_0 = const\ r_{\rm lead}/Q^2$ with $r_{\rm lead}$ standing for the ratios of leading partons over the total number of partons (2 for mesons, 3 for baryons). The (pre)hadronic expansion times t_F can be extracted from the string breaking pattern of the Lund model [36].

In Fig. 1 we present the results of our calculations. The dash-dash-dotted curves realize the CT effect in both the longitudinal and transverse channels and dash-dotted curves in the transverse channel only. In addition we show the results of the CT effect in the longitudinal channel only (dot-dot-dashed curves). As one can see, the last scenario is certainly ruled out by the present data. Because of the dominance of the transverse cross section at high values of Q^2, a use of different values of t_F in a range discussed in Ref. [33] does not change this result significantly. This is particularly interesting because presently the CT effect is expected to show up in the longitudinal channel [37].

3. *Deep exclusive π^+ electroproduction off nucleons*

An understanding of π production mechanism off nucleons is mandatory for the proof of the CT signal observed in the π electroproduction off nuclei. As we have

seen, the fate of pions in the nuclear medium depends on the initial longitudinal and/or transverse production mechanisms [33].

We first briefly describe the model for the exclusive process

$$\gamma^*(q) + N(p) \to \pi(k') + N'(p')\,, \tag{2}$$

based on exclusive-inclusive connection. Following Ref. [23], we distinguish two classes of primary collisions: the soft hadronic and the hard partonic (DIS) production of π^+. The soft hadron-exchange part of the $\gamma^* p \to n\pi^+$ amplitude is described by the exchange of Regge trajectories. However, at the invariant masses reached in the πCT experiment ($W \approx 2.2$ GeV), nucleon resonances can contribute to the 1π channel. As in Ref. [23], this is modeled by the hard interaction of virtual photons with partons (DIS) since DIS involves all possible transitions of the nucleon from its ground state to any excited state.

For the description of the reaction $p(e, e'\pi^+)n$ in DIS, a model for the hadronization process is needed. In the present description of the hadronization in DIS, we rely on the Lund fragmentation model as depicted in Fig. 2 where the leading order $\gamma^* q \to q$ DIS process followed by the fragmentation of an excited string into two particles (πN) is shown. As a realization of the Lund model, we use the

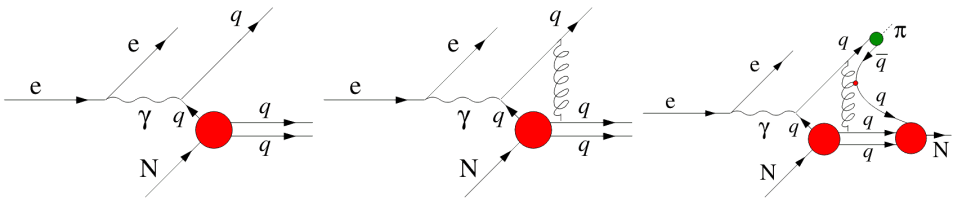

Fig. 2. A schematic representation of the partonic DIS part of the π^+-electroproduction mechanism. The wavy line represents a color string. See text for the details.

JETSET implementation. This description, which connects the exclusive and semi-inclusive DIS production in the limit $z \to 1$, resolves the longstanding puzzle of a large theoretical underestimate of the observed transverse strength in the reaction $p(e, e'\pi^+)n$ [23]. For instance, in Fig. 3 we confront the result of our calculations (solid curves) with the JLAB data [7] for unseparated cross sections at the average value of $W \simeq 2.2$ GeV. The data are very well described by the present model in the measured range from $Q^2 \simeq 1$ GeV^2 up to 5 GeV^2. Note that the high Q^2 dependence of the data essentially follows the Q^2 dependence of the deep inelastic structure functions in DIS. A strong rise at low values of Q^2 is due to the π-reggeon exchange. Its Q^2 dependence is driven by the pion charge form factor. The high Q^2 domain of the reaction is totally transverse. See Ref. [23] for further details.

Why DIS pions matter for the CT effect. A necessary condition for the CT effect is the propagation of a quark-gluon system, originating in the hard partonic interaction, through the nuclear medium and its subsequent interactions with surrounding nucleons. In the present model, the hard DIS part of the primary high energy electromagnetic interaction is determined by the Lund model which means that the

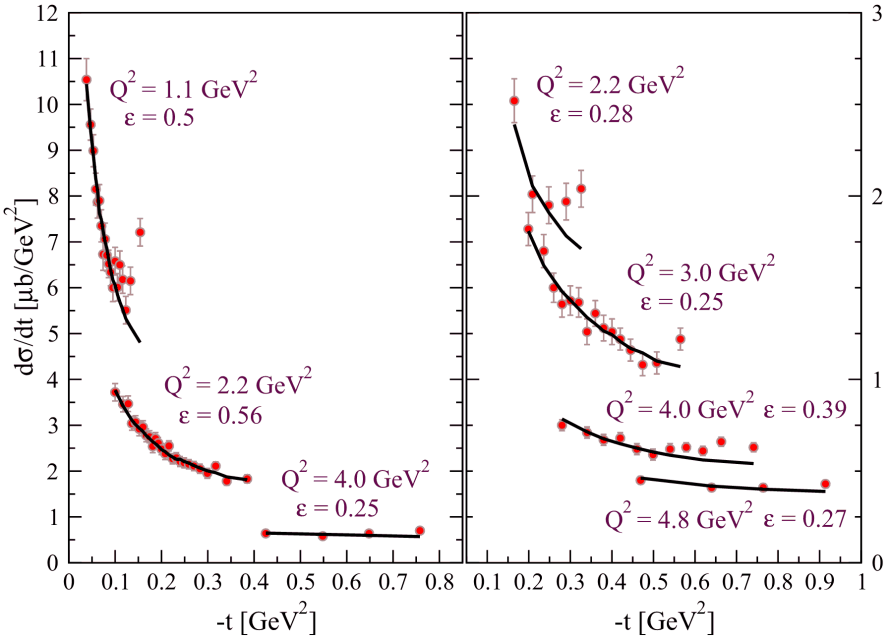

Fig. 3. Differential cross section $\mathrm{d}\sigma/\mathrm{d}t = \mathrm{d}\sigma_{\mathrm{T}}/\mathrm{d}t + \varepsilon \mathrm{d}\sigma_{\mathrm{L}}/\mathrm{d}t$ *of the reaction* $p(\gamma^*, \pi^+)n$. *The solid curves are the model predictions. The experimental data are from Ref. [7].*

final state consists of an excited string (see Fig. 2). This string then fragments into hadrons. In the exclusive reaction $(e, e'\pi^+)$ considered here, all DIS pions are – because of their high energy $z \approx 1$ – directly connected to the hard interaction point and have production time $t_P = 0$. Thus, following the Lund model hadronization pattern, the (pre)hadronic interaction in Eq. (1) is effective only for the DIS events; the longitudinal cross section, which is dominated by the π-knockout from the preexisting meson cloud of a nucleon, is not affected by this (pre)hadronic interaction. In the model of Ref. [23], only the DIS (transverse) part of the cross section is responsible for the observed CT effect since this part is connected with the 4D pattern of the string breaking dynamics which makes the formation time of produced (pre)hadrons finite. Indeed, the transverse nature of the CT effect at JLAB agrees remarkably well with data, see Fig. 1.

4. *Deep exclusive* π *electroproduction and nucleon resonances*

In Refs. [23, 24], the transverse cross section σ_{T} was modeled using the string breaking mechanism in DIS. However, the solution of the problem on the amplitude level is still missing. Both the soft hadronic and hard partonic parts of the amplitude

can in principle interfere, making non-additive contributions to $\sigma_{\rm L}$ and to interference $\sigma_{\rm TT}$ and $\sigma_{\rm LT}$ cross sections. Indeed, the data from JLAB demonstrate [3, 11] that the magnitude and sign of the interference cross sections are not compatible with the simple exchange of a pion Regge trajectory in the t-channel. Because the contributions from exchange of heavy mesons are small [23], this would suggest the presence of a large transverse resonance or partonic interfering background to the meson-pole contributions.

In Ref. [27] we attempted a phenomenological approach to model the presence of nucleon resonances beyond the t-channel meson-exchange amplitudes. We modeled the contribution of nucleon resonances using a local Bloom-Gilman connection between the exclusive and inclusive reactions.

In Fig. 4 we show the results of Ref. [27] where the excitation of nucleon resonances is taken into account. We also compare these results with the ones obtained in the previouse section, see Fig. 3, when using the concept of DIS pions. The square symbols connected by solid lines describe the model results. The data are very well reproduced by the present model in the measured Q^2 range from $Q^2 \simeq 1$ GeV^2

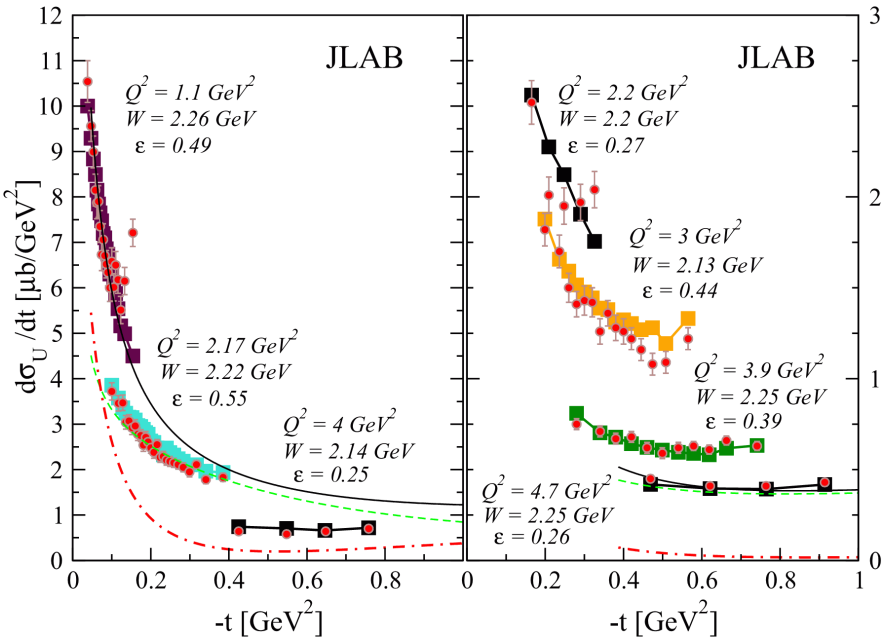

Fig. 4. The differential cross sections $\mathrm{d}\sigma_{\rm U}/\mathrm{d}t = \mathrm{d}\sigma_{\rm T}/\mathrm{d}t + \varepsilon \mathrm{d}\sigma_{\rm L}/\mathrm{d}t$ *in exclusive reaction* $p(\gamma^*, \pi^+)n$ *at JLAB [7]. The square symbols connected by solid lines describe the model results. The discontinuities in the curves result from the different values of* (Q^2, W, ε) *for the various* $(-t)$ *bins. The dash-dotted and dashed curves describe the contributions of the longitudinal* $\varepsilon \mathrm{d}\sigma_{\rm L}$ *and transverse* $\mathrm{d}\sigma_{\rm T}$ *cross sections, respectively, to the total unseparated cross sections (solid curves) for the the lowest and highest average values of* $Q^2 = 1.1$ GeV^2 *and* $Q^2 = 4.7$ GeV^2.

up to 5 GeV^2. In Fig. 4 we also show the contributions of the longitudinal $\varepsilon d\sigma_{\rm L}$ (dash-dotted curves) and transverse $d\sigma_{\rm T}$ (dashed curves) cross sections to the total unseparated cross sections (solid curves) for the lowest and highest average values of $Q^2 = 1.1$ GeV^2 and $Q^2 = 4.7$ GeV^2. The cross sections at high values of Q^2 are flat and totally transverse. At forward angles a strong peaking of the cross section at $Q^2 = 1.1$ GeV^2 comes from the large longitudinal component in this case. The off-forward region is transverse. This behavior agrees with the results from Ref. [23].

The same behavior is observed in the DIS regime at HERMES [5] where the value of W is higher. At HERMES, because of the Regge shrinkage of the π-reggeon exchange and smaller transverse component, the forward peak just has a steeper $(-t)$-dependence [24]. In Fig. 5 we show our results for the $-t + t_{\rm min}$ dependence of the differential cross section $\mathrm{d}\sigma_U/\mathrm{d}t = \mathrm{d}\sigma_{\rm T}/\mathrm{d}t + \epsilon \mathrm{d}\sigma_{\rm L}/\mathrm{d}t$ in exclusive reaction $p(\gamma^*, \pi^+)n$ at HERMES.

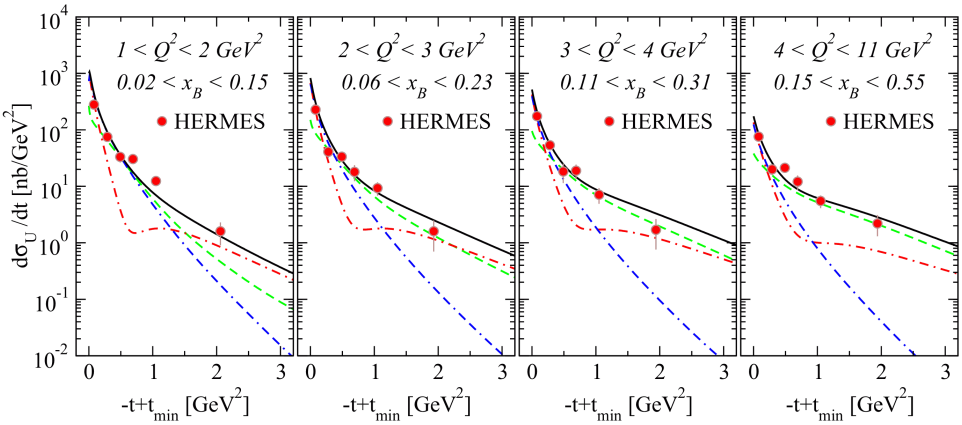

Fig. 5. $-t + t_{\rm min}$ dependence of the differential cross section $\mathrm{d}\sigma_U/\mathrm{d}t = \mathrm{d}\sigma_{\rm T}/\mathrm{d}t + \epsilon \mathrm{d}\sigma_{\rm L}/\mathrm{d}t$ in exclusive reaction $p(\gamma^*, \pi^+)n$ at HERMES. The experimental data are from Ref. [5]. The calculations are performed for the average values of $(Q^2, x_{\rm B})$ in a given Q^2 and Bjorken $x_{\rm B}$ bin. The solid curves are the full model results. The dash-dotted curves correspond to the longitudinal $\epsilon \mathrm{d}\sigma_{\rm L}/\mathrm{d}t$ and the dashed curves to the transverse $\mathrm{d}\sigma_{\rm T}/\mathrm{d}t$ components of the cross section. The dash-dash-dotted curves describe the results without the resonance/partonic effects.

In Fig. 6 we show our results for separated differential cross sections in the $p(\gamma^*, \pi^+)n$ reaction together with the high-Q^2 data from Refs. [21, 3]. The notations for the curves are described in the caption to the figure. The histograms in Fig. 6 for $\mathrm{d}\sigma_{\rm T}/\mathrm{d}t$ are the results of Ref. [23]. Our present treatment of resonance contributions produces a result which is very close to that obtained in our previous work [23]. However, the present approach goes beyond the two-component hadron-parton model of Ref. [23] and allows to study the interference and non-π-pole background effects on the amplitude level.

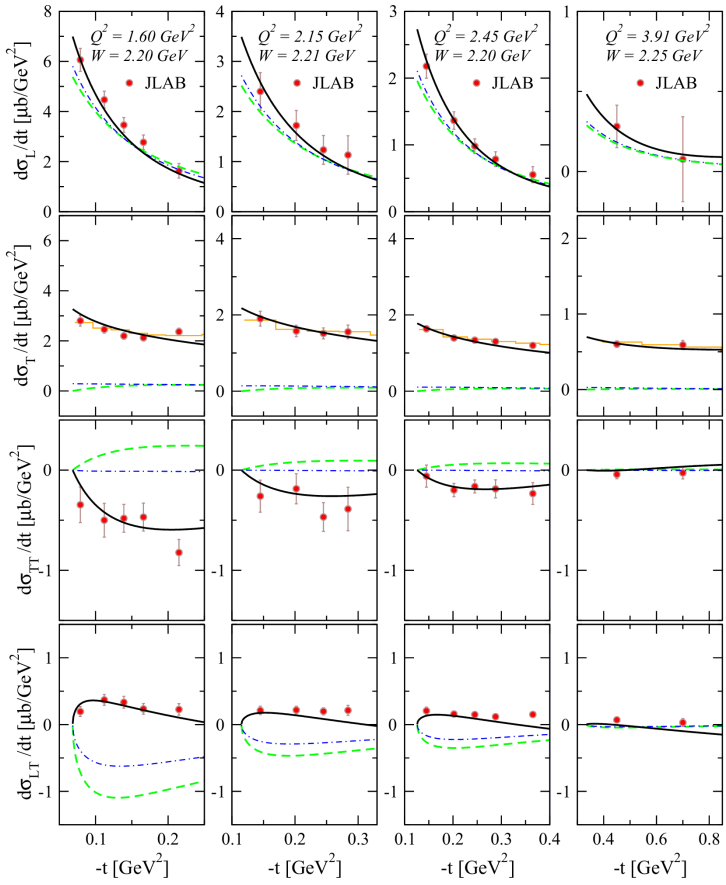

Fig. 6. $-t$ *dependence of* L/T *partial transverse* $\mathrm{d}\sigma_\mathrm{T}/\mathrm{d}t$*, longitudinal* $\mathrm{d}\sigma_\mathrm{L}/\mathrm{d}t$ *and interference* $\mathrm{d}\sigma_\mathrm{TT}/\mathrm{d}t$ *and* $\mathrm{d}\sigma_\mathrm{LT}/\mathrm{d}t$ *differential cross sections in exclusive reaction* $p(\gamma^*,\pi^+)n$*. The experimental data are from the* $F\pi$*-2 [21] and* π*-CT [3] experiments at JLAB. The numbers displayed in the plots are the average* (Q^2, W) *values. The dashed curves correspond to the exchange of the* π*-Regge trajectory alone. The dash-dotted curves are obtained with the on-mass-shell form factors in the nucleon-pole contribution and exchange of the* $\rho(770)/a_2(1320)$ *trajectory. The solid curves describe the model results with the resonance contributions. The data points in each* (Q^2, W) *bin correspond to slightly different values of* Q^2 *and* W *for the various* $-t$ *bins. The calculations are performed for values of* Q^2 *and* W *corresponding to the first* $-t$ *bin. The histograms for* $\mathrm{d}\sigma_\mathrm{T}/\mathrm{d}t$ *are the results from [23].*

5. Q^2 dependence of the cross sections

It has been proposed that the Q^2 dependence of L/T separated exclusive $p(\gamma^*,\pi^+)n$ cross sections may provide a test of the factorization theorem [2] in

the separation of long-distance and short-distance physics and the extraction of GPD. The leading twist GPD scenario predicts for $\sigma_{\rm L} \sim 1/Q^6$ and $\sigma_{\rm T} \sim 1/Q^8$. An observation of the Q^2 power law scaling is considered as a model independent test of QCD factorization.

The Q^2 behavior of cross sections in exclusive reaction $p(\gamma^*, \pi^+)n$ has been studied at JLAB in Ref. [3]. It was shown that while the scaling laws are reasonably consistent with the Q^2 dependence of the longitudinal $\sigma_{\rm L}$ data, they fail to describe the Q^2 dependence of the transverse $\sigma_{\rm T}$ data. The Q^2 dependence of the $p(\gamma^*, \pi^+)n$ cross section in DIS has been also studied at HERMES [5]. It was found that the Q^2 dependence of the data is in general well described by the calculations from GPD models which include the power corrections, see Ref. [5] and references therein. However, the magnitude of the theoretical cross section is underestimated. In the following we check this predicted $\sigma_{\rm L}/\sigma_{\rm T} \sim Q^2$ scaling within our model calculations.

In Fig. 7 (left panel) we show our results for the Q^2 dependence of $p(\gamma^*, \pi^+)n$ reaction cross sections $\mathrm{d}\sigma_{\rm L}/\mathrm{d}t$ and $\mathrm{d}\sigma_{\rm T}/\mathrm{d}t$ at fixed $-t$ and Bjorken variable x_B. The experimental data are from Ref. [3] and correspond to the forward π^+ production.

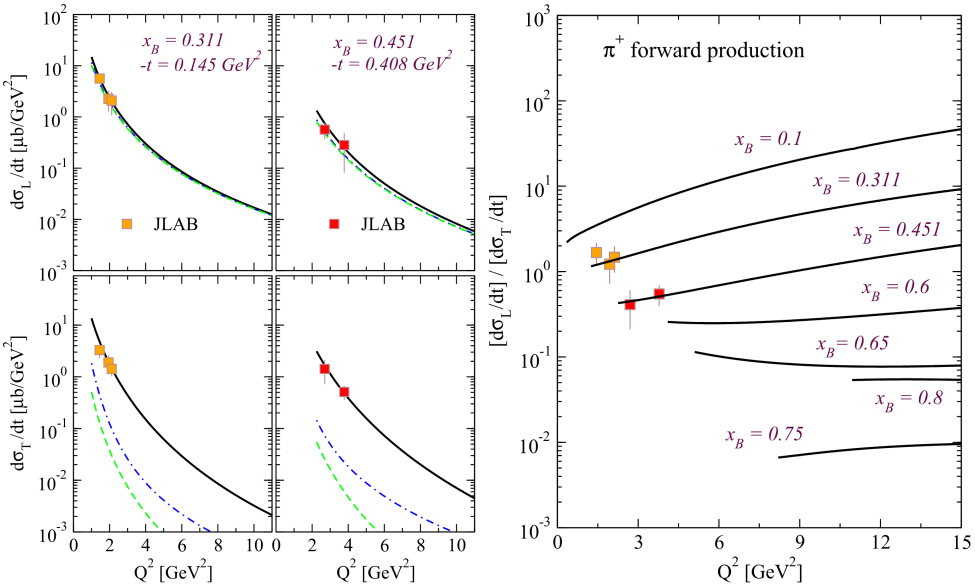

Fig. 7. Left panel: Q^2 dependence of the longitudinal $\mathrm{d}\sigma_{\rm L}/\mathrm{d}t$ (top panels) and transverse $\mathrm{d}\sigma_{\rm T}/\mathrm{d}t$ (bottom panels) cross sections in $p(\gamma^*, \pi^+)n$ reaction at fixed values of $-t$ and Bjorken $x_{\rm B}$. The solid curves are the model predictions for the scaling curves. The dashed curves correspond to the contribution of the π-reggeon exchange alone. The dash-dotted curves are the model results without the contributions of resonances. The experimental data are from Ref. [3]. Right panel: The Q^2 dependence of the ratio of longitudinal $\mathrm{d}\sigma_{\rm L}/\mathrm{d}t$ to transverse $\mathrm{d}\sigma_{\rm T}/\mathrm{d}t$ differential cross sections in the forward π^+ production. The different curves correspond to different values of Bjorken scaling variable $x_{\rm B}$.

The solid curves are the model predictions and describe the available data very well. The dashed curves describe the contribution of the π-reggeon exchange to the Q^2 scaling curves only. The dash-dotted curves are the model results without the resonance contributions. The latter effect is again large in the transverse cross section and gives only small correction to the longitudinal cross section $\mathrm{d}\sigma_\mathrm{L}/\mathrm{d}t$. The Q^2 dependence of $\mathrm{d}\sigma_\mathrm{L}/\mathrm{d}t$ is essentially driven by the pion form factor.

The Q^2 dependence of the ratio of the longitudinal $\mathrm{d}\sigma_\mathrm{L}/\mathrm{d}t$ to the transverse $\mathrm{d}\sigma_\mathrm{T}/\mathrm{d}t$ differential cross sections for the forward π^+ production is shown in Fig. 7 (right panel). The different curves correspond to different values of x_B. All curves start at the value of $W \simeq 1.9$ GeV. For small and intermediate values of x_B, the model results show an increase of the ratio $\mathrm{d}\sigma_\mathrm{L}/\mathrm{d}\sigma_\mathrm{T}$ as a function of Q^2. Only at small values of Bjorken x_B, the ratio $\mathrm{d}\sigma_\mathrm{L}/\mathrm{d}\sigma_\mathrm{T}$ is qualitatively in agreement with the predicted $\sim Q^2$ behavior. In the valence quark region above $x_\mathrm{B} \simeq 0.6$, the cross section ratio scales and is actually independent of the value of Q^2. In this region, the transverse component σ_T dominates the π^+ electroproduction cross section. In the experimental determination of the pion transition form factor from forward σ_L data, one can, therefore, better isolate the longitudinal response by minimizing the Bjorken x_B.

The physics content of the HERMES deep exclusive $p(\gamma^*, \pi^+)n$ data is essentially the same as at JLAB. Figure 8 shows the Q^2 dependence of the measured cross sections in DIS for different x_B bins [5]. These are the same data sets from HERMES (see previous section) integrated over $-t$. The Q^2 dependence of the experimental data is well described by the calculations (solid curves) from the present model. The dashed and dash-dotted curve describe the longitudinal $\varepsilon\sigma_\mathrm{L}$ and the transverse σ_T components, respectively.

In the region of small Bjorken x_B, see left panel in Fig. 8, the integrated longitudinal component dominates over the transverse cross section. With increasing x_B, the strength of the transverse component is increasing, and for values of x_B in the third bin, the transverse cross section σ_T becomes the dominant part of the exclusive cross section. An increase of the relative contribution of σ_T as a function of x_B can be clearly seen in the right panel of Figure 8 where $0.26 < x_\mathrm{B} < 0.55$. There the first Q^2 bin corresponds to the average value of $x_\mathrm{B} = 0.29$ and the last Q^2 bin to the average value of $x_\mathrm{B} = 0.44$.

6. Beam single spin asymmetry (SSA)

We further consider the electroproduction reaction

$$\vec{e} + N \to e' + \pi + N, \tag{3}$$

and now assume that the target nucleon is unpolarized, whereas we allow arbitrary polarization for the incoming electron. With a polarized beam $\vec{e}$ and with an unpolarized target there is an additional component $\sigma_{\mathrm{LT}'}$ [27] in the $(e, e'\pi)$ cross section which is proportional to the imaginary part of an interference between the L/T photons and therefore sensitive to the relative phases of amplitudes.

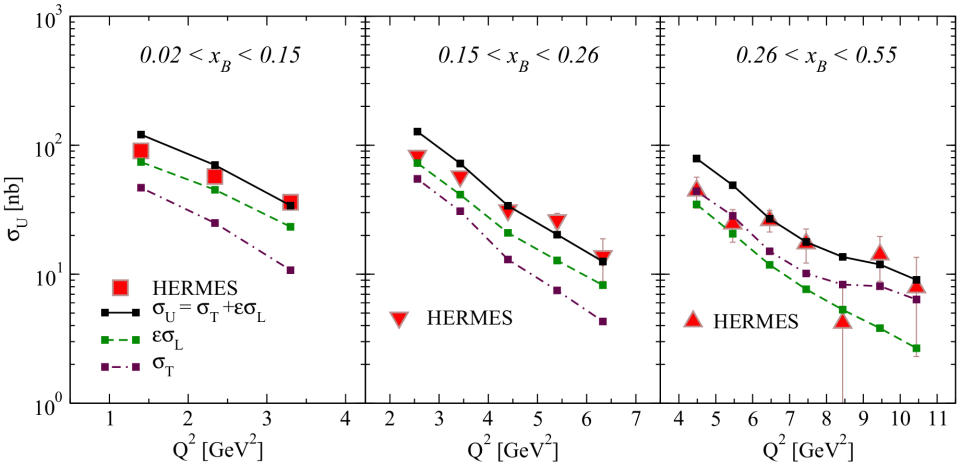

Fig. 8. Q^2 dependence of the integrated cross sections $\sigma_{\rm U} = \sigma_{\rm T} + \epsilon\sigma_{\rm L}$ in exclusive reaction $p(\gamma^*, \pi^+)n$ at HERMES. The different panels correspond to different x_B bins. The solid curves are the model results. The dashed and dash-dotted curves correspond to the longitudinal $\epsilon\sigma_{\rm L}$ and transverse $\sigma_{\rm T}$ components of the cross section, respectively. The experimental data are from Ref. [5].

Using the polarized electron beam, the longitudinal beam single-spin asymmetry (SSA) in $N(\vec{e}, e'\pi)N'$ scattering is defined so that

$$A_{\rm LU}(\phi) \equiv \frac{d\sigma^{\rightarrow}(\phi) - d\sigma^{\leftarrow}(\phi)}{d\sigma^{\rightarrow}(\phi) + d\sigma^{\leftarrow}(\phi)}, \tag{4}$$

where $d\sigma^{\rightarrow}$ refers to positive helicity $h = +1$ of the incoming electron. The azimuthal moment associated with the beam SSA is given by

$$A_{\rm LU}^{\sin(\phi)} = \frac{\sqrt{2\varepsilon(1-\varepsilon)}d\sigma_{\rm LT'}}{d\sigma_{\rm T} + \varepsilon d\sigma_{\rm L}}. \tag{5}$$

In general, a nonzero $\sigma_{\rm LT'}$ or the corresponding beam SSA $A_{\rm LU}(\phi)$, Eq. (4), demands interference between single helicity flip and nonflip or double helicity flip amplitudes. In Regge models the asymmetry may result from Regge cut corrections to single reggeon exchange. This way the amplitudes in the product acquire different phases and therefore relative imaginary parts. A nonzero beam SSA can be also generated by the interference pattern of amplitudes where particles with oppositeparities are exchanged.

In the left panel of Fig. 9 we plot the CLAS data [28] for the azimuthal moment $A_{\rm LU}^{\sin(\phi)}$ associated with the beam SSA, Eq. (5), in the reaction $p(\vec{e}, e'\pi^+)n$. These data have been collected in hard scattering kinematics $E_e = 5.77$ GeV, $W > 2$ GeV and $Q^2 > 1.5$ GeV^2. The experiment shows a sizable and positive beam SSA.

In the left and right panels of Fig. 9 we present our results for the azimuthal moments $A_{\rm LU}^{\sin(\phi)}$ in the reactions $p(\vec{e}, e'\pi^+)n$ and $n(\vec{e}, e'\pi^-)p$, respectively.

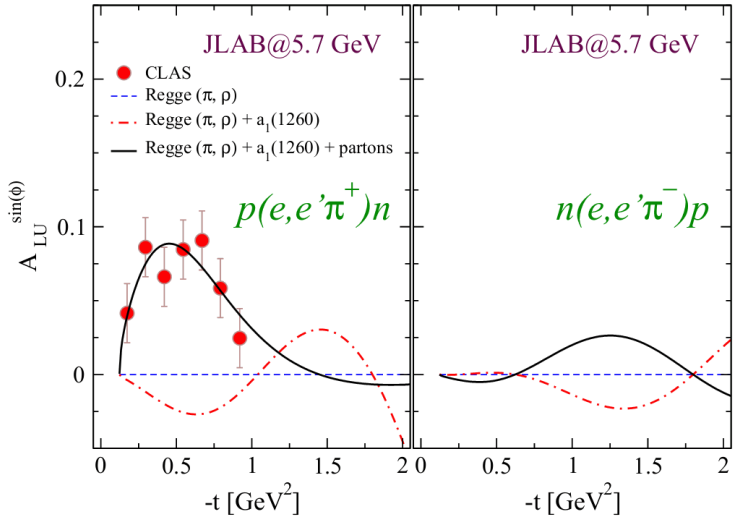

Fig. 9. Left panel: The beam spin azimuthal moment $A_{\rm LU}^{\sin(\phi)}$ *in exclusive reaction* $p(\gamma^*,\pi^+)n$ *as a function of* $-t$*. The CLAS/JLAB data are from [28]. The dashed curves describe the results (the asymmetry is zero) without the resonance contributions and neglecting the exchange of unnatural parity* $a_1(1260)$ *Regge trajectory. The dash-dotted curves correspond to the addition of the axial-vector* $a_1(1260)$*-reggeon exchange. The solid curves are the model results and account for the resonance/partonic effects. Right panel: The beam spin azimuthal moment* $A_{\rm LU}^{\sin(\phi)}$ *in exclusive reaction* $n(\gamma^*,\pi^-)p$*.*

We first consider $A_{\rm LU}^{\sin(\phi)}$ generated by the exchange of Regge trajectories. In Fig. 9, the dashed curves describe the model results without the effects of resonances and neglecting the exchange of the axial-vector $a_1(1260)$ Regge trajectory. This model results in a zero $A_{\rm LU}^{\sin(\phi)}$ and therefore a zero beam SSA. The addition of the unnatural parity $a_1(1260)$-exchange generates by the interference with the natural parity $\rho(770)$ exchange a sizable $A_{\rm LU}^{\sin(\phi)}$ in both channels. This result corresponds to the dash-dotted curves in Fig. 9. In the rest of unpolarized observables discussed above, the effect of the axial-vector $a_1(1260)$ is small. However, as one can see, the contribution of $a_1(1260)$ is important in the polarization observables. For instance, a strong interference pattern of the $a_1(1260)$-reggeon exchange makes the polarization observables, like the beam SSA, very sensitive to the different scenarios describing the structure and behavior of $a_1(1260)$ in high-Q^2 processes. In the last step we account for the resonance contributions. The latter strongly influence the asymmetry parameter $A_{\rm LU}^{\sin(\phi)}$. The model results (solid curves) are in agreement with the positive $A_{\rm LU}^{\sin(\phi)}$ in the π^+ channel and predict much smaller $A_{\rm LU}^{\sin(\phi)}$ in the π^- channel. A sizable and positive $A_{\rm LU}^{\sin(\phi)}$ has been also observed at HERMES in π^+ SIDIS close to the exclusive limit $z \to 1$ [29].

As in deep exclusive π^+ electroproduction, a sizeable and positive beam

SSA has recently been measured at CLAS/JLAB also in the exclusive reaction $p(\vec{e}, e'\pi^0)p$ [38]. It was shown that the simple Regge model used in [38] fails to explain the measured kinematic $(\sqrt{s}, Q^2)$ dependencies. We have, therefore, extended our calculation of Ref. [27] to the neutral pion channel. In the Regge exchange contributions, the vector $\omega(782)$ and axial-vector $b_1(1235)$ and $h_1(1170)$ trajectories are taken into account. We find that at high values of Q^2 the dominant contribution to the beam SSA again comes from the residual excitation of nucleon resonances. Our results are shown in Fig. 10 and describe the JLAB data very well.

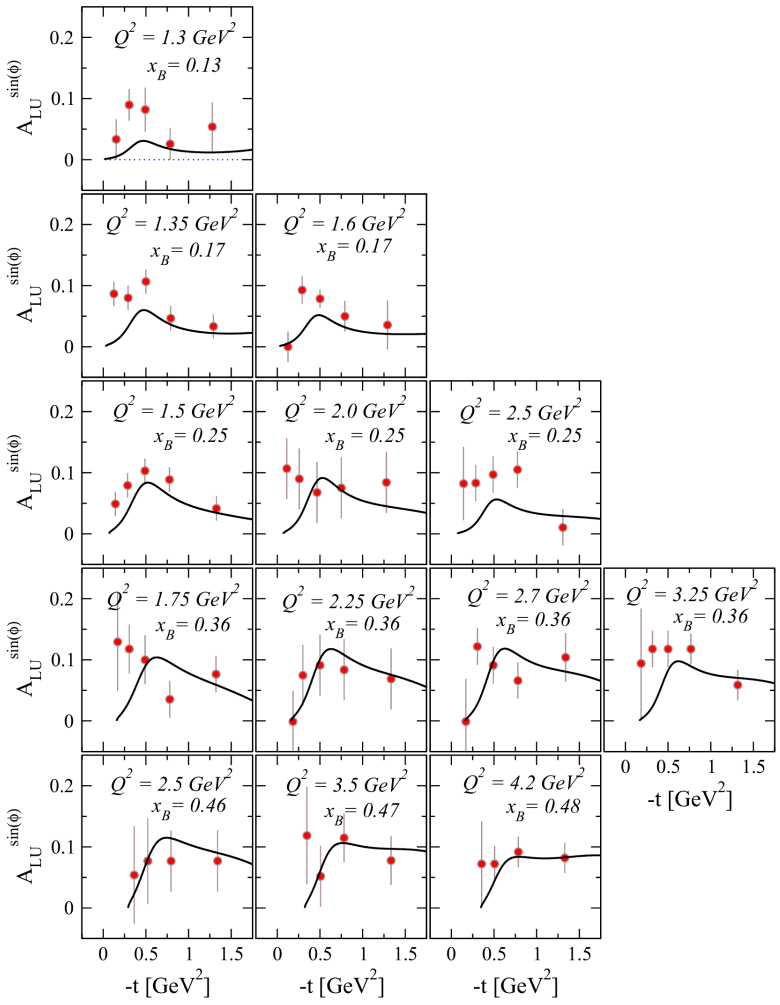

Fig. 10. The beam spin azimuthal moment $A_{\rm LU}^{\sin(\phi)}$ in exclusive reaction $p(\gamma^*, \pi^0)p$ as a function of $-t$ for different $(Q^2, x_{\rm B})$ bins. The solid curves are the model results and account for the residual effect of nucleon resonances. The experimental data are from Ref. [38].

7. Summary

In the first part of this work we present a calculation of the nuclear transparency of pions in the reaction $A(e, e'\pi^+)A^*$ off nuclei. The microscopic input for the primary interaction of the virtual photon with the nucleon describes both the transverse and the longitudinal cross sections. The coupled-channel BUU transport model has been used to describe the FSI of hadrons in the nuclear medium. The formation times of (pre)hadrons follow the time-dependent hadronization pattern of hard DIS processes. Our results are consistent with the JLAB data and show that a detailed understanding of the primary $\gamma^* N$ interaction is essential for a quantitative understanding (and proof) of CT.

In the second part of the work we describe different approaches to exclusive production of pions off nucleons. We propose a resolution of the $\sigma_{\rm T}$ problem in the reaction $p(e, e'\pi^+)n$ above the resonance region. It is based on the concept of DIS pions and combines the meson-exchange currents and DIS of virtual photons off partons. Following a two-component hadron-parton picture of Refs. [23, 24], we further develop a model which combines a Regge-pole approach with residual effects of nucleon resonances. The contribution of nucleon resonances has been assumed to be dual to direct partonic interaction and therefore describes the hard part of the model cross sections. The resonance/partonic effects are taken into account using a Bloom-Gilman connection between the exclusive hadronic form factors and inclusive deep inelastic structure functions. The model results agree well with the experimental data measured at JLAB and DESY.

Acknowledgements

This work was supported by DFG through TR16 and by BMBF.

References

[1] C. Weiss, *Proceedings of 18th International Spin Physics Symposium (SPIN 2008)*, AIP Conf. Proc. **1149** (2009) 150; [arXiv:0902.2018 [hep-ph]].

[2] J. C. Collins, L. Frankfurt and M. Strikman, Phys. Rev. D **56** (1997) 2982.

[3] T. Horn et al., Phys. Rev. C **78** (2008) 058201.

[4] E. Fuchey et al., arXiv:1003.2938 [nucl-ex].

[5] A. Airapetian et al., Phys. Lett. B **659** (2008) 486.

[6] A. Airapetian et al., Phys. Lett. B **682** (2010) 345.

[7] X. Qian et al., Phys. Rev. C **81** (2010) 055209.

[8] E. D. Bloom and F. J. Gilman, Phys. Rev. D **4** (1971) 2901.

[9] E. D. Bloom and F. J. Gilman, Phys. Rev. Lett. **25** (1970) 1140.

[10] V. Tadevosyan et al., Phys. Rev. C **75** (2007) 055205.

[11] H. P. Blok et al., Phys. Rev. C **78** (2008) 045202.

[12] P. Brauel et al., Phys. Lett. B **65** (1976) 184; Phys. Lett. B **69** (1977) 253.

[13] H. Ackermann et al., Nucl. Phys. B **137** (1978) 294.

[14] P. Brauel et al., Z. Phys. C **3** (1979) 101.
[15] C. J. Bebek et al., Phys. Rev. D **9** (1974) 1229.
[16] C. J. Bebek et al., Phys. Rev. D **13** (1976) 25.
[17] C. J. Bebek et al., Phys. Rev. D **17** (1978) 1693.
[18] C. N. Brown et al., Phys. Rev. D **8** (1973) 92.
[19] J. D. Sullivan, Phys. Lett. B **33** (1970) 179.
[20] V. G. Neudatchin et al., Nucl. Phys. A **739** (2004) 124.
[21] T. Horn et al., Phys. Rev. Lett. **97** (2006) 192001.
[22] G. M. Huber et al., Phys. Rev. C **78** (2008) 045203.
[23] M. M. Kaskulov, K. Gallmeister and U. Mosel, Phys. Rev. D **78** (2008) 114022.
[24] M. M. Kaskulov and U. Mosel, Phys. Rev. C **80** (2009) 028202.
[25] J. D. Bjorken and J. Kogut, Phys. Rev. D **8** (1973) 1341.
[26] K. Gallmeister, M. Kaskulov and U. Mosel, Phys. Rev. C **83** (2011) 015201; [arXiv:1007.1141 [hep-ph]].
[27] M. M. Kaskulov and U. Mosel, Phys. Rev. C **81** (2010) 045202.
[28] H. Avakian and L. Elouadrhiri [CLAS Collaboration], Phys. Part. Nucl. **35** (2004) S114.
[29] A. Airapetian et al., Phys. Lett. B **648** (2007) 164.
[30] B. Clasie et al., Phys. Rev. Lett. **99** (2007) 242502.
[31] A. Larson, G. A. Miller and M. Strikman, Phys. Rev. C **74** (2006) 018201.
[32] W. Cosyn, M. C. Martinez and J. Ryckebusch, Phys. Rev. C **77** (2008) 034602.
[33] M. M. Kaskulov, K. Gallmeister and U. Mosel, Phys. Rev. C **79** (2009) 015207.
[34] For details of the GiBUU method see: http://gibuu.physik.uni-giessen.de/GiBUU.
[35] G. R. Farrar et al., Phys. Rev. Lett. **61** (1988) 686.
[36] K. Gallmeister and T. Falter, Phys. Lett. B **630** (2005) 40.
[37] M. Strikman, arXiv:0711.1625 [hep-ph].
[38] R. De Masi et al. [CLAS Collaboration], Phys. Rev. C **77** (2008) 042201.

EKSKLUZIVNA ELEKTROTVORBA PIONA NA NUKLEONIMA I JEZGRAMA

Izlažemo ishode svojih računa za ekskluzivnu elektrotvorbu piona na nukleonima i jezgrama za visoke vrijednosti Q^2. Razmatramo pojavu prozirnosti (CT) za boje koju su opazili nedavno u JLabu u elektrotvorbi $A(e, e'\pi)$ na jezgrama. Pokazujemo da je opis tvorbe π obvezatan za dokaz CT podatka iz JLaba. Zatim razvijamo model za ekskluzivnu tvorbu π na nukleonima u JLabu i HERMESu. Prvo opisujemo model zasnovan na spoju ekskluzivno-inkluzivno. U drugom pristupu spajamo metodu Reggeovih polova s učinkom dalekih nukleonskih rezonancija. Nukleonske rezonancije opisujemo rabeći dvojni spoj ekskluzivnih faktora oblika i strukturnih funkcija duboko neelastičnih inkluzivnih procesa. Opisujemo i ishode mjerenja azimutalnih asimetrija spina snopa iz JLaba u ekskluzivnoj elektrotvorbi nabijenih i neutralnih piona.